SCIENCE CHINA
Chemistry

•ARTICLES•

December 2019 Vol.62 No.12: 1720–1724
https://doi.org/10.1007/s11426-019-9605-0

Single-atom electrocatalysis: a new approach to *in vivo* electrochemical biosensing

Hanfeng Hou[1†], Junjie Mao[4†], Yunhu Han[3], Fei Wu[2], Meining Zhang[1*], Dingsheng Wang[3], Lanqun Mao[2*] & Yadong Li[3]

[1]*Department of Chemistry, Renmin University of China, Beijing 100872, China;*
[2]*Beijing National Laboratory for Molecular Sciences, Key Laboratory of Analytical Chemistry for Living Biosystems, Institute of Chemistry, Chinese Academy of Sciences, Beijing 100190, China;*
[3]*Department of Chemistry, Tsinghua University, Beijing 100084, China;*
[4]*Key Laboratory of Functional Molecular Solids, Ministry of Education, Anhui Key Laboratory of Molecule-Based Materials, College of Chemistry and Materials Science, Anhui Normal University, Wuhu 241000, China*

Received June 11, 2019; accepted September 5, 2019; published online October 21, 2019

Modulation of interfacial electron transfer has been proven to pave a new approach to *in vivo* electrochemical monitoring of brain chemistry; however, designing and establishing highly efficient electrocatalytic scheme towards neurochemicals remain a long-standing challenge. Here, we find that recently established single-atom catalyst (SAC) can be used for catalyzing the electrochemical process of physiologically relevant chemicals and thus offers a new avenue to *in vivo* electrochemical biosensing. To prove this new concept, we used Co single-atom catalyst (Co-SAC), in which the atomic active sites are dispersed in ordered porous N-doping carbon matrix at atomic level, as an example of SACs for analyzing glucose as the physiologically relevant model chemicals. We found that Co-SAC catalyzes the electrochemical oxidation of hydrogen peroxide (H_2O_2) at a low potential of ca. +0.05 V (vs. Ag/AgCl). This property was further used for developing an oxidase-based glucose biosensor that was used subsequently as a selective detector of an online electrochemical system (OECS) for continuous monitoring of microdialysate glucose in rat brain. The OECS with Co-SAC-based glucose biosensor as the online detector was well responsive to glucose without interference from other electroactive species in brain microdialysate. This study essentially offers a new approach to *in vivo* electrochemical analysis with SACs as electrocatalysts to modulate interfacial electron transfer.

single-atom catalyst, *in vivo* analysis, electrocatalysis, biosensor

Citation: Hou H, Mao J, Han Y, Wu F, Zhang M, Wang D, Mao L, Li Y. Single-atom electrocatalysis: a new approach to *in vivo* electrochemical biosensing. *Sci China Chem*, 2019, 62: 1720–1724, https://doi.org/10.1007/s11426-019-9605-0

1 Introduction

Physiological and pathological processes in the central nervous system (CNS) are basically encoded by neuromodulators, neurotransmitters and other kinds of neurochemicals among neurons [1]. Thus, development of analytical mechanisms and tools that can *in vivo* monitor neurochemicals remain essential to investigating chemical nature underlying brain function. Electrochemistry has proven excellent capability of *in vivo* analysis in terms of its high spatiotemporal resolution, and diverse signal readout such as potential, current and resistance [2,3]. However, the chemical complexity of the cerebral environment largely necessitates a capability of the method in well differentiating the neurochemicals of interest from others in the CNS.

To solve the problem mentioned above, some strategies have been employed, which can generally fall into two categories [2]. One is to use different electrochemical techni-

†These authors contributed equally to this work.
*Corresponding authors (email: mnzhang@ruc.edu.cn; lqmao@iccas.ac.cn)

ques, such as differential pulse voltammetry and fast-scan cyclic voltammetry to differentiate the potentials for the redox process of neurochemicals with similar electron transfer rates. The other is to use selective recognition elements such as enzymes and aptamers to fabricate biosensors for *in vivo* recognition of neurochemicals. Over the past decade, we have been demonstrating that modulating electron transfer kinetics and ion transport behavior could pave a new and effective avenue to *in vivo* monitoring of brain chemistry [1,4–9]. For example, we found that the use of carbon nanotubes (CNTs) greatly facilitated the oxidation of ascorbic acid at a low potential that is well separated from those of other neurochemicals. This finding eventually enabled *in vivo* analysis of ascorbic acid under various physiological and pathological processes with a high selectivity and reliability [10–12].

Since its first report in 2011, single-atom electrocatalysts have received extensive attention because of their maximum atom utilization, superior reactivity and selectivity [13]. They not only exhibit excellent performance in electrocatalysis but also show high stability because their catalytic active sites are mostly dominated by the surface atoms. These active atoms are embedded in the supporting substrate through covalent bonds or coordination bonds, and thus the catalysts face fewer challenges in migration and agglomeration that normally occur in nanoparticle electrocatalysts [14–18]. In this regard, single-atom electrocatalysts have been widely used for electrocatalytic oxygen reduction, hydrogen evolution, CO_2 reduction, CO oxidation and so on [19–24]. However, as far as we know, there is no report on the use of single-atom electrocatalysts to develop an analytical method for *in vivo* monitoring of brain chemistry.

In this study, we describe the first demonstration on the use of single-atom electrocatalysts (SAC; e.g., Co-SAC) to develop an analytical method for *in vivo* monitoring of neurochemicals (i.e., glucose). We find that Co-SAC exhibits good electrocatalytic activity toward the oxidation of H_2O_2. This property is further employed to fabricate an oxidase-based glucose biosensor and thereby an online electrochemical system to continuously monitor glucose in the microdialysate of rat brain. This study essentially demonstrates a new approach to *in vivo* electrochemical biosensing, which is envisaged to be of great importance in understanding molecular basis underlying brain functions.

2 Experimental

2.1 General materials and reagents

SBA-15 was purchased from JCNANO Technology Co., Ltd. (China). Cobalt(II) chloride hexahydrate ($CoCl_2·6H_2O$), 2,2′-bipyridine, cobalt(II) nitrate hexahydrate, 2-methylimidazole and sodium hydroxide were obtained from Sinopharm Chemical (China). Co-SAC was synthesized as reported previously [25]. Ascorbic acid (AA), uric acid (UA), dopamine (DA), dihydroxy-phenyl acetic acid (DOPAC), bovine serum albumin (BSA), D-(+)-glucose, glutaraldehyde and glucose oxidase were purchased from Sigma-Aldrich and used without further purification. Artificial cerebrospinal fluid (aCSF, pH 7.4) consists of NaCl (126 mM), KCl (2.4 mM), KH_2PO_4 (0.5 mM), $MgCl_2$ (0.85 mM), $NaHCO_3$ (27.5 mM), Na_2SO_4 (0.5 mM), and $CaCl_2$ (1.1 mM). All other chemicals were of at least analytical grade. All solutions were prepared with deionized water (Milli-Q, Millipore, USA).

2.2 Instrument and measurements

All *in vitro* electrochemical experiments and online electrochemical measurements were conducted in a three-electrode cell at room temperature using a computer-controlled potentiostat (CHI 660e, China), similar to our previous work [26]. A 10 μL of Co-SAC dispersion solution (1 mg/mL) was drop-cast onto glassy carbon (GC) electrodes to obtain Co-SAC-modified electrodes. After being air-dried, 5 μL of employing glucose oxidase (GOx) solution (10 mg/mL), 2 μL of BSA (1 wt%) and 1 μL of glutaraldehyde solution (1 wt%) were mixed thoroughly and dropped on the Co-SAC layer to form GOx/Co-SAC-modified GC electrodes. The electrodes were dried and further coated with 1 μL Nafion (0.5% in ethanol). The resulting electrodes were dried at room temperature for about 30 min before measurements. Transmission electron microscopy (TEM) and aberration corrected high-angle annular dark-field scanning transmission electron microscope (AC HAADF-STEM) images were recorded on a JEOL-2100F FETEM (Japan) with electron acceleration energy of 200 kV.

2.3 *In vivo* microdialysis and online electrochemical measurements

Adult male rats (350–400 g) purchased from the Experimental Animal Center of Peking University were served as subjects. The rats were housed on a light-dark schedule (12/12 h) with food and water *ad libitum*. All the animal experiments were conducted according to the Institutional Animal Care and Use Committee of National Center for Nanoscience and Technology of China. Surgery for *in vivo* microdialysis was performed as reported previously [27–29]. Briefly, microdialysis guide cannulas were carefully implanted in the striatum (anteroposterior (AP)=0 mm, mediolateral (*L*)=3 mm from bregma, dorsoventral (*V*)=3.5 mm from dura) using standard stereotaxic procedures. The microdialysate was continuously sampled and directly detected in an electrochemical flow cell with a microinjection pump (CMA 100, CMA Microdialysis AB, Sweden) perfusing aCSF at a flow rate of 3 μL/min.

3 Results and discussion

The surface structure and morphology of Co-SAC was investigated by TEM and AC HAADF-STEM. As confirmed by Figure 1(a, b), Co-SAC maintains the ordered porous structure of SBA-15. At the sub-angstrom resolution, Co atoms can be identified as the brighter spots dispersed over the darker surface of the N-doped carbon substrate. Element mapping of Co-SAC demonstrates the homogeneous distributions of Co and N atoms throughout the carbonaceous matrix (Figure 1(d)). This is in accordance with our previous observation of the atomic form of Co anchored in solid substrates by X-ray absorption fine structure measurements [25]. Each Co atom coordinates to four N atoms with no Co–Co bond forming, and the valence of Co is between Co^0 and Co^{2+} [25].

Cyclic voltammetry (CV) was performed with Co-SAC-modified, N-doped carbon substrate-modified and bare GC electrodes to assess their electrocatalytic activities toward H_2O_2. As shown in Figure 2(a), at the Co-SAC-modified GC electrode, well-defined anodic and cathodic peaks were recorded at +0.05 and −0.02 V (vs. Ag/AgCl), and the peak currents increase with increasing the concentration of H_2O_2, indicating that the peaks were ascribed to the oxidation and reduction of H_2O_2, respectively. In comparison, N-doped carbon substrate-modified GC electrode exhibits lower activity in catalyzing the electro-reduction of H_2O_2 due to a 100 mV negative shift of its onset potential and retarded current increase as an indication of slower electron transfer kinetics (cathodic peak at –0.27 V, Figure 2(b)). Oxidative peak of H_2O_2 was also missing without the presence of Co atoms (Figure 2(b)) and at GC electrode (Figure 2(c)). It should be mentioned that oxygen was also reducible at the Co-SAC-modified GC electrode, reflected by a small cathodic peak at ca. −0.02 V in air-saturated solution (Figure 2(d)), which might be the reason why the cathodic peak current is larger than the anodic one. In order to further ensure that the peak current was contributed to H_2O_2, we added catalase into aCSF containing 4 mM H_2O_2 to selectively catalyze H_2O_2 into O_2 and H_2O. As can be seen in Figure 2(e), both the anodic and cathodic currents decrease, again suggesting that Co-SAC is the excellent electrocatalyst in activation of H_2O_2 in both directions. Unlike the anodic peak, the cathodic peak still exists due to the reduction of oxygen.

It is worth mentioning herein that this is the first observation of such an electrocatalytic property toward the transformations of H_2O_2 with non-noble metal and carbon materials. Although Co ions host in porphyrins can electrocatalyze the reduction of H_2O_2 at −0.3 V, it shows no activity toward the reversed oxidation reaction, as reported previously [30]. The commonly used Pt electrode catalyzes the electro-oxidation of H_2O_2 at higher potential, typically above

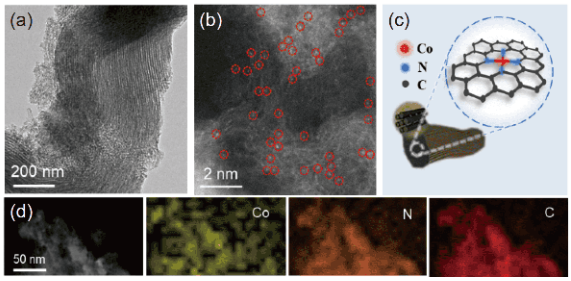

Figure 1 (a) TEM image of Co-SAC; (b) AC HAADF-STEM image of Co-SAC with Co atoms identified in red circles; (c) illustration of the structure of Co-SAC, C (grey), N (blue) and Co (red); (d) EDX mapping of Co-SAC (color online).

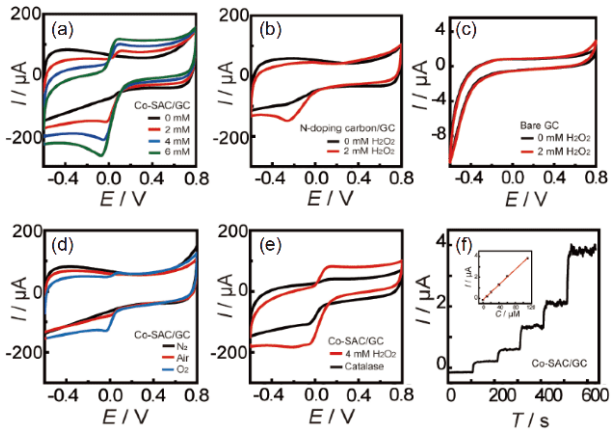

Figure 2 Typical cyclic voltammograms (CVs) obtained with (a) Co-SAC-modified GC electrode in air-saturated aCSF (pH 7.4) containing 0, 2, 4, and 6 mM H_2O_2, (b) N-doped carbon substrate-modified and (c) bare GC electrodes in air-saturated aCSF (pH 7.4) in the absence (black curve) and presence of 2 mM H_2O_2 (red curve), (d) Co-SAC-modified GC electrode in aCSF (pH 7.4) saturated with N_2 (black curve), ambient air (red curve), or O_2 (blue curve), (e) Co-SAC-modified GC electrode in air-saturated aCSF (pH 7.4) containing 4 mM H_2O_2 in the absence (red curve) and presence of 0.5 mg/mL catalase (black curve). Scan rate, 100 mV/s. (f) Amperometric response recorded at the Co-SAC-modified GC electrode toward successive additions of 10, 10, 20, 20 and 50 μM H_2O_2 into air-saturated aCSF (pH 7.4). Inset: plot of the current intensity as a function of H_2O_2 concentration. Potential, +0.20 V (vs. Ag/AgCl) (color online).

+0.4 V [31]. The high electrocatalytic performance might be ascribed to the unique structure of Co-SAC, which is different with the Co particle. As reported previously, the valence of Co atom in Co-SAC is between 0 and +2 and the binding energy of OH species to the single Co site in SAC is smaller than that of OH species to Co particle [25,32]. These properties of Co atom in Co-SAC might be the reason of the high electrocatalytic performance observed here because the metal–OH remains critical for the oxidation of H_2O_2 [33].

In order to avoid the interference of oxygen, we used the electrocatalytic oxidation process to investigate the performance of Co-SAC-modified GC electrode in electrochemical sensing of H_2O_2. Figure 2(f) shows the amperometric response of the Co-SAC-modified GC electrode poised at +0.20 V toward the successive addition of H_2O_2. Staircase

current elevation upon H_2O_2 titration produces a linear relationship between the current intensity and the concentration of H_2O_2 up to 110 μM with a sensitivity of 35.1 nA/μM. This is comparable with those of Pd-based and Pt-based H_2O_2-oxidizing sensors, but the latter sensors were typically operated at higher potentials (i.e., +0.6 V) (Table 1).

Stepping forward, we established a cascade scheme on working electrode of a glucose biosensor, by GOx as the biorecognition unit and Co-SAC as the electrocatalyst for H_2O_2 produced by enzymatic glucose oxidation. The biosensor was then polarized at +0.20 V to detect glucose without the interference from other electroactive species coexisting in the brain. Similar amperometric responses toward glucose titration were obtained with the as-prepared glucose sensor, delivering current signals linearly at glucose concentration in the range of 5.0 μM–1 mM with a sensitivity of 1.02 nA/μM (Figure 3(a)). Temporal resolution and sensing stability of the GOx/Co-SAC-based glucose biosensor were also evaluated. It can be seen from Figure 3(b) that the biosensor generates a fast current increase upon the addition of glucose, and then the current level for glucose remains unchanged in the presence of 0.50 mM glucose for more than 1 h, indicating the applicability of the biosensor in continuous measurements of glucose. The good stability of the Co-SAC-based biosensor may be related to the structure of Co-SAC, in which each atom of Co is anchored on the substrate by four N atoms to prevent aggregation at longer timescale and thus maintain high catalytic activity.

In order to validate the GOx/Co-SAC-based biosensor for continuously monitoring the dynamics of glucose *in vivo*, it was integrated in an online electrochemical system (OECS), whose sensitivity and selectivity were systematically investigated *in vitro*. Figure 4(a) depicts the typical amperometric responses obtained with the GOx/Co-SAC-based OECS toward glucose with aCSF as the perfusion solution. The system was well responsive toward the perfusion of glucose when the biosensor was polarized at a constant potential of +0.20 V (vs. Ag/AgCl). In the subsequent test, common coexisting electroactive species were perfused into the system at their respective physiological levels (0.1 μM UA, 5 μM AA, 0.1 μM DA, and 0.1 μM DOPAC). No obvious current responses were yielded with these interferents,

Table 1 Comparison of our Co-SAC/GC sensor with other H_2O_2-oxidizing sensors

Electrode design	Conditions (V vs. Ag/AgCl)	Sensitivities (nA/μM)	Refs.
Pt-NPs/CNT/GC	0.6	3.9	[34]
Pd-NPs/GC	0.6	40.3	[35]
MnO_2/Na-montmorillonite/GC	0.65	2.2	[36]
MnO_2/Nafion/GC	0.8	35.3	[37]
Co-SAC/GC	0.2	35.1	This work

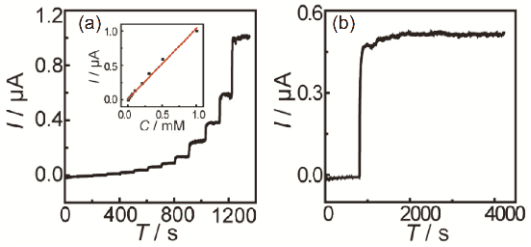

Figure 3 (a) Amperometric response of the GOx/Co-SAC-based biosensor toward successive additions of different concentrations of glucose. Inset: plot of the current response as a function of glucose concentration. (b) Amperometric response of the biosensor toward titration of 0.50 mM glucose in aCSF (pH 7.4). The electrode was polarized at +0.20 V (vs. Ag/AgCl) (color online).

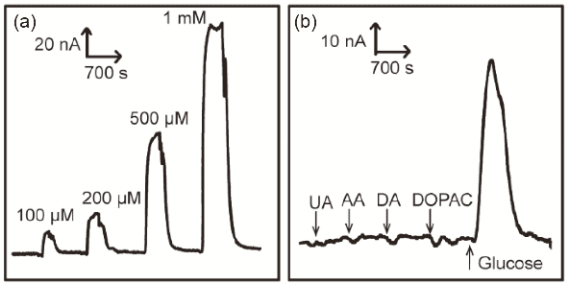

Figure 4 (a) Typical amperometric responses obtained with OECS using GOx/Co-SAC-based biosensor as the detector toward continuous perfusion of glucose at different concentrations of 100 μM, 200 μM, 500 μM, and 1 mM into the system. (b) Typical amperometric responses obtained with the OECS toward perfusion of UA (0.1 μM), AA (5 μM), DA (0.1 μM), DAOPAC (0.1 μM) and glucose (200 μM) in aCSF (pH 7.4). The biosensor was polarized at +0.20 V. Flow rate, 3 μL/min.

until 200 μM glucose was added and gave rise to a relatively large current response. These results suggest that the GOx/Co-SAC-based OECS may be applied for selective measurement of glucose in rat brain.

The GOx/Co-SAC-based OECS was finally validated for *in vivo* monitoring of glucose in the microdialysate continuously sampled from rat striatum (Figure 5(a)). As shown in Figure 5(b), current intensity delivered by the OECS increases upon contact with the microdialysate continuously sampled out and reaches a plateau that corresponds to the basal level of glucose estimated to be ca. 120 μM. The change of the microdialysate glucose level was evoked by the intraperitoneal injection of insulin (5 U), resulting in a large current decrease due to promoted consumption of blood glucose in the brain. These results are consistent with the previous reports [29,38]. Taken together, the GOx/Co-SAC-based OECS was demonstrated to be able to track the dynamics of glucose in the brain.

4 Conclusions

In summary, we have demonstrated that Co-SAC exhibits

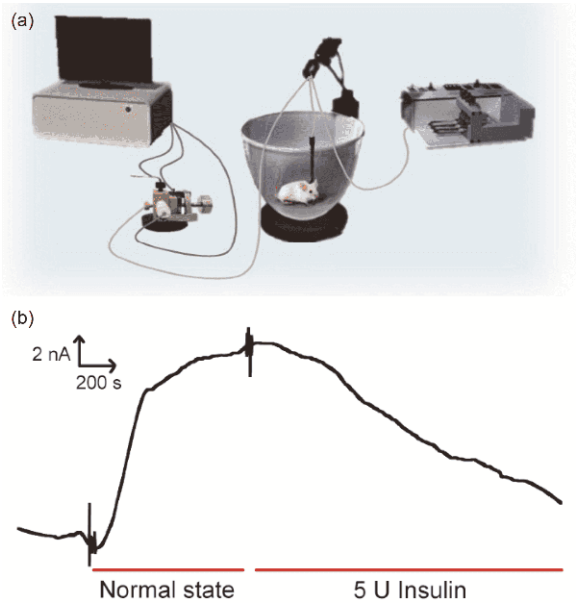

Figure 5 (a) Schematic of OECS with the GOx/Co-SAC-based biosensor for continuous monitoring of glucose in the brain of rats. (b) Typical amperometric responses of the OECS toward the microdialysate sampled from rat striatum under normal state and after intraperitoneal injection of 5 U insulin. The biosensor was polarized at +0.20 V. Flow rate, 3 μL/min (color online).

excellent electrocatalytic property to the oxidation of H_2O_2 and can be used for developing enzymatic biosensors with oxidases as biorecognition elements. The prepared GOx/Co-SAC-based OECS shows sensitive, selective and stable amperometric response to glucose in brain microdialysate. We envisage that Co-SAC used here could also be applied in designing other oxidase-based biosensors for *in vivo* biosensing of neurochemicals such as lactate and glutamate in the CNS. Therefore, this study essentially indicates that SAC opens a new avenue to modulating the electron transfer of electroactive species, offering a new approach to *in vivo* analysis of brain chemistry with high accuracy.

Acknowledgements This work was supported by the National Natural Science Foundation of China (21790390, 21790391, 21621062, 21435007, 21874152), the National Basic Research Program of China (2016YFA0200104) and the Chinese Academy of Sciences (QYZDJ-SSW-SLH030).

Conflict of interest The authors declare that they have no conflict of interest.

1 Zhang M, Yu P, Mao L. *Acc Chem Res*, 2012, 45: 533–543
2 Xiao T, Wu F, Hao J, Zhang M, Yu P, Mao L. *Anal Chem*, 2017, 89: 300–313
3 Robinson DL, Hermans A, Seipel AT, Wightman RM. *Chem Rev*, 2008, 108: 2554–2584
4 Wu F, Yu P, Mao L. *Chem Soc Rev*, 2017, 46: 2692–2704
5 Li R, Liu X, Qiu W, Zhang M. *Anal Chem*, 2016, 88: 7769–7776
6 Guo S, Yan H, Wu F, Zhao L, Yu P, Liu H, Li Y, Mao L. *Anal Chem*, 2017, 89: 13008–13015
7 Zhang K, He X, Liu Y, Yu P, Fei J, Mao L. *Anal Chem*, 2017, 89: 6794–6799
8 He X, Zhang K, Li T, Jiang Y, Yu P, Mao L. *J Am Chem Soc*, 2017, 139: 1396–1399
9 Yan H, Guo S, Wu F, Yu P, Liu H, Li Y, Mao L. *Angew Chem Int Ed*, 2018, 57: 3922–3926
10 Zhang M, Liu K, Gong K, Su L, Chen Y, Mao L. *Anal Chem*, 2005, 77: 6234–6242
11 Zhang M, Liu K, Xiang L, Lin Y, Su L, Mao L. *Anal Chem*, 2007, 79: 6559–6565
12 Xiao T, Wang Y, Wei H, Yu P, Jiang Y, Mao L. *Angew Chem Int Ed*, 2019, 58: 6616–6619
13 Qiao B, Wang A, Yang X, Allard LF, Jiang Z, Cui Y, Liu J, Li J, Zhang T. *Nat Chem*, 2011, 3: 634–641
14 Wang A, Li J, Zhang T. *Nat Rev Chem*, 2018, 2: 65–81
15 Liu L, Corma A. *Chem Rev*, 2018, 118: 4981–5079
16 Liu J, Jin Z, Wang X, Ge J, Liu C, Xing W. *Sci China Chem*, 2019, 62: 669–683
17 Huang P, Liu W, He Z, Xiao C, Yao T, Zou Y, Wang C, Qi Z, Tong W, Pan B, Wei S, Xie Y. *Sci China Chem*, 2018, 61: 1187–1196
18 Fang Z, Yu G. *Sci China Chem*, 2018, 61: 1045–1046
19 Chen Y, Ji S, Wang Y, Dong J, Chen W, Li Z, Shen R, Zheng L, Zhuang Z, Wang D, Li Y. *Angew Chem*, 2017, 129: 7041–7045
20 Chen W, Pei J, He CT, Wan J, Ren H, Zhu Y, Wang Y, Dong J, Tian S, Cheong WC, Lu S, Zheng L, Zheng X, Yan W, Zhuang Z, Chen C, Peng Q, Wang D, Li Y. *Angew Chem Int Ed*, 2017, 56: 16086–16090
21 Pan Y, Lin R, Chen Y, Liu S, Zhu W, Cao X, Chen W, Wu K, Cheong WC, Wang Y, Zheng L, Luo J, Lin Y, Liu Y, Liu C, Li J, Lu Q, Chen X, Wang D, Peng Q, Chen C, Li Y. *J Am Chem Soc*, 2018, 140: 4218–4221
22 Nie L, Mei D, Xiong H, Peng B, Ren Z, Hernandez XIP, DeLaRiva A, Wang M, Engelhard MH, Kovarik L, Datye AK, Wang Y. *Science*, 2017, 358: 1419–1423
23 Mao J, He CT, Pei J, Chen W, He D, He Y, Zhuang Z, Chen C, Peng Q, Wang D, Li Y. *Nat Commun*, 2018, 9: 4958
24 Ma W, Mao J, Yang X, Pan C, Chen W, Wang M, Yu P, Mao L, Li Y. *Chem Commun*, 2019, 55: 159–162
25 Han Y, Wang Z, Xu R, Zhang W, Chen W, Zheng L, Zhang J, Luo J, Wu K, Zhu Y, Chen C, Peng Q, Liu Q, Hu P, Wang D, Li Y. *Angew Chem Int Ed*, 2018, 57: 11262–11266
26 Lin Y, Liu K, Yu P, Xiang L, Li X, Mao L. *Anal Chem*, 2007, 79: 9577–9583
27 Lin Y, Li B, Hao J, Xiao T, Yang Y, Yu P, Mao L. *Electrochim Acta*, 2016, 209: 132–137
28 Liu K, Yu P, Lin Y, Wang Y, Ohsaka T, Mao L. *Anal Chem*, 2013, 85: 9947–9954
29 Wang X, Li Q, Xu J, Wu S, Xiao T, Hao J, Yu P, Mao L. *Anal Chem*, 2016, 88: 5885–5891
30 Chan RJH, Su YO, Kuwana T. *Inorg Chem*, 1985, 24: 3777–3784
31 Westbroek P, Haute BV, Temmerman E. *Anal BioAnal Chem*, 1996, 354: 405–409
32 Han Y, Wang YG, Chen W, Xu R, Zheng L, Zhang J, Luo J, Shen RA, Zhu Y, Cheong WC, Chen C, Peng Q, Wang D, Li Y. *J Am Chem Soc*, 2017, 139: 17269–17272
33 Katsounaros I, Schneider WB, Meier JC, Benedikt U, Biedermann PU, Auer AA, Mayrhofer KJJ. *Phys Chem Chem Phys*, 2012, 14: 7384–7391
34 You T, Niwa O, Tomita M, Hirono S. *Anal Chem*, 2003, 75: 2080–2085
35 Niwa O, Kato D, Kurita R, You T, Iwasaki Y, Hirono S. *Sensor Mater*, 2007, 19: 225–233
36 Yao S, Yuan S, Xu J, wang Y, Luo J, Hu S. *Appl Clay Sci*, 2006, 33: 35–42
37 Zhang L, Fang Z, Ni Y, Zhao G. *Int J Electrochem Sci*, 2009, 4: 407–413
38 Ma W, Jiang Q, Yu P, Yang L, Mao L. *Anal Chem*, 2013, 85: 7550–7557